Published in final edited form as:

Cancer Res. 2017 February 01; 77(3): 672–683. doi:10.1158/0008-5472.CAN-16-1765.

Human Pancreatic Cancer Cells Induce a MyD88-Dependent Stromal Response To Promote a Tumor-Tolerant Immune Microenvironment

Daniel Delitto[1], **Andrea E. Delitto**[2], **Bayli B. DiVita**[2], **Kien Pham**[3,5], **Song Han**[1], **Emily R. Hartlage**[2], **Brittney N. Newby**[3], **Michael H. Gerber**[1], **Kevin E. Behrns**[1], **Lyle L. Moldawer**[1], **Ryan M. Thomas**[1], **Thomas J. George Jr.**[4], **Todd M. Brusko**[3], **Clayton E. Mathews**[3], **Chen Liu**[3,5], **Jose G. Trevino**[1], **Steven J. Hughes**[1,*], and **Shannon M. Wallet**[2,*]

[1]Department of Surgery, University of Florida, Gainesville, FL, USA

[2]Department of Oral Biology, University of Florida, Gainesville, FL, USA

[3]Department of Pathology, Immunology, Laboratory Medicine, University of Florida, Gainesville, FL, USA

[4]Department of Medicine, University of Florida, Gainesville, FL, USA

[5]Department of Pathology and Laboratory Medicine, Rutgers New Jersey Medical School and Rutgers Robert Wood Johnson Medical School, Newark, NJ, USA

Abstract

Cancer cells exert mastery over the local tumor-associated stroma (TAS) to configure protective immunity within the tumor microenvironment. The immunomodulatory character of pancreatic lysates of patients with cancer differs from those with pancreatitis. In this study, we evaluated the crosstalk between pancreatic cancer (PC) and its TAS in primary human cell culture models. Upon exposure of TAS to PC cell-conditioned media, we documented robust secretion of IL-6 and IL-8. This TAS response was MyD88-dependent and sufficient to directly suppress both CD4+ and CD8+ T cell proliferation, inducing Th17 polarization at the expense of Th1. We found that patients possessed a similar shift in circulating effector memory Th17:Th1 ratios compared to healthy controls. The TAS response also directly suppressed CD8+ T cell-mediated cytotoxicity. Overall, our results demonstrate how TAS contributes to the production of an immunosuppressive tumor microenvironment in pancreatic cancer.

Introduction

Pancreatic cancer (PC) is projected to be the second leading cause of cancer deaths by 2030, in large part due to resistance to current systemic therapies (1). Recent discoveries have challenged the notion that PC has poor antigenicity, suggesting that the local

[*]**Co-Corresponding Authors**: Shannon M. Wallet, Department of Oral Biology, University of Florida, College of Dentistry, PO BOX 100434, Gainesville, FL 32610, USA, swallet@dental.ufl.edu, Steven J. Hughes, MD, Department of Surgery, University of Florida College of Medicine, PO BOX 100109, Gainesville, FL 32610, USA, steven.hughes@surgery.ufl.edu.

Conflicts of Interest: None

microenvironment contributes to the protection of tumor cells from host immune recognition (2). The mechanisms proposed in generating this protection have implicated the early infiltration of the microenvironment by regulatory immune cell subsets (2). Recently, PC therapies have been designed to take advantage of this knowledge by inducing antitumor immune responses. While several of these immunotherapies have achieved promising results in preclinical models (3), these findings have not translated into success in human trials (4). Thus, the current challenge in the field is to translate these findings into the human disease, which mandates knowledge of the immunological microenvironment specific to humans as well as the mechanisms that are responsible for the observed phenotype(s). Here we delineate one mechanism of how the tumor microenvironment contributes to the suppression of antitumor immune responses in humans.

Innate immunity is triggered not only by recognition of pathogen associated molecular patterns (PAMPs) but also by endogenous alarmins released upon injury and cell death (DAMPs). Sensing of these stimuli occurs through a myriad of pattern recognition receptors (PRRs), the result of which shapes and determines the intensity and direction of the adaptive immune response. The intensity and polarization of this response determines the balance between tumor cell killing and tolerance (5). Although innate immunity is generally beneficial to the host, an over-exuberant or persistent response can result in tissue injury (6). To minimize this possibility, the immune system is equipped with negative regulatory mechanisms that suppress inflammation and down-regulate adaptive immunity. These latter mechanisms are commonly usurped by the cancer microenvironment to permit tumor growth and tissue invasion (6).

Many tumors express “neoantigens” derived from somatic mutations that can be recognized by T cells. Upon recognition of a neoantigen, the naïve $CD8^+$ T cell population can be transformed into antitumor cytotoxic T cells through their cytokine profile, perforin/granzyme effector molecules and CD95/CD95L interactions (7). Yet, even in the face of an active $CD8^+$ T cell response, established tumors progress, indicating immunosuppressive mechanisms are at play that antagonize T cell-mediated antitumor immunity (6). In this context, $CD4^+$ T cell skewing can be critical, which can also be heavily influenced by the tumor microenvironment (6,8–10).

Inflammatory responses in the tumor microenvironment are generally accompanied by the recruitment of fibroblasts and the induction of fibrosis (6). This tumor-associated stroma (TAS) is responsible for deposition of collagen and various extracellular matrix components that stimulate cancer cell proliferation and angiogenesis. However, TAS also possesses poorly understood and underappreciated functions that allow it to respond to the microenvironment and shape immune responses (11). For instance, cell death within the tumor microenvironment results in the release of numerous DAMPs (5) that stimulate PRRs as well as the release of cytokines and chemokines, which can ultimately promote tumor survival and progression (12). Importantly, these DAMP-mediated processes affect not only immune cells within the tumor microenvironment, but stromal and epithelial cells as well (5,13,14). Using primary human cell culture systems, we discovered a MyD88-dependent TAS response to PC cell secreted factors that results in a pro-tumor polarization of the $CD4^+$ T cell compartment and inhibition of cytotoxicity within the $CD8^+$ T cell compartment (15–

17). These *in vitro* findings recapitulate both the intratumoral milieu and peripheral T cell profiles observed in patients with PC. Taken together, these data suggest that modulation of this TAS response would be beneficial in combination with current immunotherapeutic approaches to PC.

Materials and Methods

Surgical patient cohort

Attainment of all biospecimens and patient data were compliant with an institutional review board-approved (IRB) protocol at the University of Florida (UF). Informed consent was obtained from all patients. Resected tissue were isolated from patients who underwent surgery for benign pancreatic lesions, chronic pancreatitis and PC as previously described (18). Immediately adjacent tissues were preserved in formalin for histological verification of pathology. Additionally, peripheral blood was collected from either healthy controls or patients with PC after which plasma and mononuclear cells were isolated using a Ficoll-Paque PLUS gradient (GE Healthcare Life Sciences, Little Chalfont, United Kingdom).

Primary cell culture

Patient-derived PC cell lines were isolated from patient-derived xenografts as previously described (16,17). Epithelial cell purity was confirmed by expression of HLA ABC, EpCam and cytokeratins 18 and 19 (Biolegend, San Diego, CA). Patient-derived tumor associated stroma (TAS) cell lines were generated as previously described (15). Cell purity was confirmed by uniform expression of α-smooth muscle actin (R&D Systems, Minneapolis, MN) by flow cytometry and immunocytochemistry. Both PC and TAS cell lines were maintained and stimulated in growth medium [Dulbecco's Modified Eagle's Medium/F12 (DMEM/F12) Advanced (Life Technologies, Carlsbad, CA), 10% fetal bovine serum (FBS) (Atlanta Biologicals, Atlanta, GA), 4 mM GlutaMAX™ (Life Technologies), 20 ng/mL human epidermal growth factor (Life Technologies), Primocin™ (Invivogen, San Diego, CA) and antibiotic antimycotic solution (Sigma)] in 5% CO2/95% air at 37°C.

TAS Stimulation Assays

Primary PC cell conditioned media (PCCM) was generated by culturing 10^5 PC cells/well in 500 μL of growth medium on 24 well plates. Cells were allowed to adhere for 12 hours, after which growth medium was changed and conditioned media collected 24 hours later. 10^5 TAS cells were treated with PCCM or ultrapure LPS (Invivogen) for 24 hours and the resulting supernatants evaluated for soluble mediator concentrations. For LPS binding and TLR4 inhibition assays, polymyxin B and CLI-095 (Invivogen) were applied with either LPS or PCCM stimulation. In some experiments, knockdown of target genes was achieved using siRNA transfection. TAS were reverse transfected using either TLR4, MyD88, or IRAK1-specific or control siRNA (20 nM) in Opti-MEM® supplemented media with Lipofectamine® RNAiMAX (Thermo Fisher Scientific) for 24 hours and allowed to rest for an additional 24 hours in growth medium prior to further stimulation. In some experiments, TAS were stimulated in the presence of 10 μM of the inhibitors of IRAK4 (EMD Millipore) or IRAK1/4 (Caymen Chemicals, Ann Arbor, Michigan). In additional experiments, TAS were stimulated with 100 ng/mL of ultrapure ligands to TLR1/2, TLR2/6, TLR2, TLR3,

TLR4, TLR5, TLR7/8, TLR9, NOD1 and NOD2 (Invivogen). Concentration of ligands was chosen based on preliminary data generated using the Multi-TLR Array™ (Invivogen). Recombinant β-defensin 2 (Peprotech, Rocky Hill, NJ) and high mobility group box 1 (HMGB1) (Biolegend) were also used for TAS PRR stimulation. In additional experiments, boiling and filtering were performed by either boiling PCCM at 100°C for 20 minutes and allowing it to return to room temperature or filtering PCCM through a 0.22 μm filter, respectively, prior to TAS stimulation.

Enzyme-linked immunoassay (ELISA)

Resected pancreatic tissue, patient plasma, and tissue culture supernatants were probed for IL6 (BD Biosciences, Franklin Lakes, NJ), IL8 (BD Biosciences) and/or pro-collagen Iα1 (R&D Systems) using an ELISA and a standard curve according to the manufacturer's protocol. Resected pancreatic tissue was placed in cell lysis buffer (Cell Signaling Technologies, Danvers, MA) with a protease inhibitor cocktail (Sigma-Aldrich, St. Louis, MO). Tissues were mechanically dissociated and homogenized using the FastPrep-24 system according to the manufacturer's protocol (MP Biomedicals, Santa Ana, CA). Soluble mediator concentrations were then converted to pg/mg of tissue as follows: pg/ml of mediator divided by mg/ml of total protein, determined using the DC™ Protein Assay (BioRad, Hercules, CA).

T cell stimulations

Human T cells were magnetically sorted from a healthy donor using a commercially available, negative selection kit under the manufacturer's instructions (Stem Cell Technologies, Vancouver, Canada). 10^5 cells/well were labelled with CellTrace® Violet (Thermo Fisher Scientific) and seeded in 96 well plates in 200 μL growth medium with 50 ng/mL IL2 (PeproTech). T cells were stimulated with anti-CD3/CD28/CD137 coated beads at a 1:10 bead:cell ratio (Thermo Fisher Scientific) for 96 hours. Experimental conditions included adding either 50 μL growth medium (control), 50 μL TAS conditioned media (TAS CM), 50 μL LPS/PCCM-prestimulated TAS conditioned media ($TAS^{LPS}CM/TAS^{PC}CM$) with and without siRNA knockdown of TLR4, MyD88 or IRAK1 in TAS. Additional conditions included treatment of T cells with mouse IgG1 isotype control antibodies, mouse anti-human IL6 or mouse anti-human IL8 (R&D Systems). Cells were harvested after 96 hours and flow cytometry performed using standardized immunophenotyping panels (19). Proliferation index was defined as the average number of divisions of each T cell.

Cell-mediated lymphotoxicity assays

$CD8^+$ T cells obtained from a healthy HLA-A*02-01 donor were transduced using a lentiviral vector encoding a MART1-specific TCR, which was a generous gift donated by Richard Koya (20). Primary PC cells isolated as previously described (16,17), were evaluated for HLA A2 expression using flow cytometry with a commercially validated antibody (Biolegend) and a representative HLA A2-positive line was chosen. 2.5×10^4 PC cells were seeded in 96 well plates and allowed to adhere overnight in growth medium. Transgenic T cells were added at the indicated effector:target T cell ratio in the presence and absence of the recombinant MART1 peptide (12.5 μM, ProImmune Ltd., Oxford, United Kingdom). Images were collected on an EVOS FL digital inverted microscope (Life

Technologies, Carlsbad, CA) and processed with ImageJ (NIH). The CellTracker™ Blue (CMAC) dye was used to label T cells and co-cultures were performed in the presence of SYTOX® Green for live cell imaging (Thermo Fisher Scientific).

Flow cytometry

For TAS surface marker analysis, cells were dissociated from 24-well culture dishes using Accutase® cell detachment solution (Sigma), washed in PBS containing 10% FBS and probed for HLA ABC (APC-Cy7) and PDL1 (PE-Cy7). Manufacturer's recommended isotype controls were used as negative controls for all antibodies used. Peripheral blood mononuclear cells were isolated by Ficoll-Paque PLUS gradient (GE Healthcare Life Sciences, Little Chalfont, United Kingdom) and probed for live vs. dead, CD3, CD4, CD45RA, CCR7, CCR6 and CXCR3 using the following reagents: Live/dead yellow (Thermo Fisher Scientific, Waltham, MA), allophycocyanin (APC)-Cy7 conjugated CD3, phycoerythrin (PE) conjugated CD4, Pacific Blue™ conjugated CD45RA, Fluorescein isothiocyanate (FITC) conjugated CCR7, APC conjugated CCR6 and PE-Cy7 conjugated CXCR3. Phenotypic analysis following T cell stimulations additionally incorporated Alexa Fluor® 647 conjugated CD8, APC-Cy7 conjugated CCR6, FITC conjugated FoxP3, Peridinin-chlorophyll protein complex (PerCP)-Cy5.5 conjugated Ki67, PE-Cy7 conjugated IFNγ, PE conjugated perforin and FITC conjugated granzyme B. Apoptosis assays were performed by staining first with PE-Cy7 conjugated EpCam and then with Pacific Blue conjugated Annexin V and propidium iodide. T cell stimulations with neutralization of IL6 or IL8 were evaluated using Sytox® Green rather than live/dead yellow. All antibodies were obtained from Biolegend and staining was performed at a 1:100 dilution. Intracellular staining was performed using BD Cytofix/Cytoperm™ (BD Biosciences) according to the manufacturer's protocol. Data were acquired using a BD LSR II (BD Biosciences) and data were analyzed using FlowJo data analysis software (FLOWJO LLC, Ashland, OR).

Real-time PCR

Total RNA from unstimulated TAS cultures was harvested using an RNeasy extraction kit (Qiagen, Valencia, CA). RNA was reverse transcribed to generate cDNA and primers specific for 18rRNA and human TLRs 1–9 (SABiosciences, Frederick, MD) along with SsoAdvanced™ SYBR Green Supermix (BioRad) were used for qPCR. Standard curves were used to determine mRNA transcript copy number in individual reactions. Data were collected using CFX Connect (BioRad) and analyzed using CFX Manager™ Software (BioRad). Data were normalized to 18rRNA.

Statistical analysis

Statistical analyses were performed using SPSS version 23.0 (IBM SPSS Statistics for Windows; IBM Corp). For clinical data, all continuous variables were assessed for normality using the Shapiro-Wilk test. Normally distributed variables were compared using independent samples *t* tests. All other continuous variables were compared using the Mann-Whitney U test for two groups and Spearman's rho for correlations. Significance was determined at $P < 0.05$.

Results

The desmoplastic response in pancreatic cancer is associated with the production of IL6 and IL8

Circulating concentrations of IL8 and IL6 have been identified as diagnostic and prognostic markers for both pancreatitis and PC (21). We first confirmed that higher concentrations of both IL8 and IL6 were observed in the plasma of PC patients compared to that of healthy controls (Fig. 1A). Attention was then turned to the PC microenvironment, which is characterized by the recruitment of fibroblasts and the induction of fibrosis (6). While this TAS response is widely recognized for initiating the deposition of collagen and various extracellular matrix components, it is also critical in shaping the immune microenvironment (11). Surgically resected pancreatic tissue lysates from individuals with pancreatitis or PC were probed for the concentrations of TAS-associated pro-collagen Iα1, as well as the prognostic inflammatory mediators IL8 and IL6. PC specimens demonstrated higher concentrations of pro-collagen Iα1 when compared to healthy pancreatic lysates and those from individuals with chronic pancreatitis (Fig. 1B). Similarly, confirming observations in a separate preliminary data set (18), PC specimens also demonstrated higher concentrations of IL8 when compared to those from pancreatitis or healthy pancreas (Fig. 1B). In contrast, no significant difference was observed in the concentrations of IL6 in PC lysates compared to lysates obtained from individuals with chronic pancreatitis, although a trend was observed between the presence of PC and higher concentrations of IL6 (Fig. 1B). IL6 concentrations within PC lysates did correlate with IL8 concentrations (Fig. 1C), and the concentration of pro-collagen correlated with tissue concentrations of both IL8 and IL6 (Fig. 1C). Together these data suggest an association between the degree of desmoplasia and microenvironmental IL8 and IL6 secretion.

Tumor-associated stroma secretes IL8 and IL6 in response to pancreatic cancer cell conditioned media

TAS and PC cells work in concert to establish a pro-tumor microenvironment (22). Although TAS represents up to 80% of PC specimens by mass (23), the focus to date centers on the role of the PC cell in establishing the immune microenvironment. Thus, in order to assess TAS contributions to the unique tumor immune microenvironment, validated primary human cell culture models of TAS and PC cells were employed (Fig. 2A) (15–17). Specifically, the human TAS response to PC cell secreted factors was assessed through conditioned media transfers (Fig. 2A). TAS cultures from three different donors were treated with a 1:1 dilution of conditioned media from three additional primary PC cell donors. Regardless of TAS or PC cell patient donor, TAS cultures exhibited a robust IL8 and IL6 secretory response to PC cell conditioned media (PCCM) and the magnitude of the response appeared more dependent upon the source of PCCM than the source of TAS (Fig. 2B and C). IL8 and IL6 protein concentrations in PCCM were significantly lower compared to stimulated TAS (Fig. 2B and C). Finally, serial dilutions of PCCM with growth media confirmed that both the IL8 and IL6 response occurred in a dose-dependent fashion (Fig. 2D). Together these data indicate that TAS produces a secretory response *in vitro* to soluble factors from PC epithelial cells that parallels the local inflammatory milieu observed *in vivo*.

Secretion of IL8 and IL6 by TAS in response to pancreatic cancer cell conditioned media is MyD88-dependent

Danger associated molecular patterns (DAMPs) are released during tumor development and progression, which engage PRRs on both immune and non-immune cell populations, including TAS (24). Thus, to explore potential mechanisms leading to the observed enhanced IL8 and IL6 expression, TAS cultures were stimulated with ultrapure ligands for known PRRs. Of the twelve ligands tested, IL8 and IL6 expression was reproducibly induced by the ligation of only two PRRs (Fig. 3A and B). Specifically, ligation of TLR4 and TLR5 by either lipopolysaccharide from *E. coli* (LPS) or flagellin from *S. typhimuirium* (FLA-ST), respectively, induced secretion of both IL6 and IL8 in TAS from three different donors (Fig. 3A and B). Functional data are consistent with qPCR data demonstrating TLR4 and TLR5 expression in TAS (Supplemental Fig. S1A). The most robust response by far was observed following TLR4 ligation (Fig. 3A and B). This TAS-specific TLR4 response was dose-dependent and could be induced with as little as 1 ng/ml of LPS. Maximal responses to both TLR4 and TLR5 ligands was observed at 100 ng/ml of LPS (Fig. 3C and D) and 100 ng/mL of FLA-ST (Supplemental Fig. S1B). Given the robust response to TLR4, TAS were then stimulated by recombinant TLR4-binding DAMPs. No significant IL6 secretion was observed with either high mobility group box 1 (HMGB1) or β-defensin 2 (Supplemental Fig. S1, C and D).

To elucidate whether the IL6 and IL8 response induced by PCCM was dependent on innate immune signaling, siRNA knockdown and pharmacologic inhibition of the TLR signaling pathway were performed in TAS cultures. With the exception of TLR3, TLR ligation induces a MyD88-dependent cascade of signaling that converges on the interleukin-1 receptor associated kinase (IRAK) family members, including IRAK1 and IRAK4 (25). Thus, siRNA knockdown of TLR4, MyD88 or IRAK1 was performed and confirmed based on reduced ultrapure LPS-mediated IL6 induction (Fig. 4A). siRNA knockdown of TLR4 ameliorated IL6 induction only at 10% PCCM, while both MyD88 and IRAK1 knockdown strongly inhibited the IL6 response at higher concentrations of PCCM (Fig. 4B). Knockdown of either MyD88 or IRAK1 also inhibited PCCM-induced IL8 secretion (Supplemental Fig. S1, E and F). TAS cultures were also treated with IRAK4 or IRAK1/4 inhibitors prior to exposure to PCCM. Inhibition of signaling was again confirmed based on reduced LPS-mediated IL6 induction (Fig. 4C). Both IRAK4 and IRAK1/4 inhibition ameliorated the PCCM-mediated IL6 induction (Fig. 4D). Similarly, TAS cultures treated with CLI-095, an inhibitor of TLR4 via its intracellular domain, resulted in inhibition of LPS- and PCCM-stimulated IL6 secretion (Fig. 4E). Intriguingly, a higher dose of CLI-095 was required to inhibit PCCM-induced IL6 secretion compared to LPS, suggesting potential nonspecific TLR inhibition. No increase in apoptosis was observed in TAS following exposure to CLI-095, IRAK4 or IRAK1/4 inhibitors at the indicated doses (data not shown). As these PCCM-mediated responses mirrored that of LPS, the absence of endotoxin contamination was confirmed using polymyxin B, which binds and sequesters the lipid A region of endotoxin. Indeed, polymyxin B only effectively inhibited LPS-stimulated IL6 secretion, while PCCM-stimulated IL6 secretion was unaffected (Fig. 4F). We further observed that the PCCM responses were due to a heat labile molecule (Fig. 4G) that was not removed upon filtration with a 0.22 μm filter (Fig. 4H). Together these demonstrate that

PCCM-induced expression of IL6 by TAS is MyD88-dependent and implicate TLR4 activation as a contributing factor.

Pancreatic cancer cell conditioned media induces the upregulation of antigen presentation machinery on TAS in the context of negative co-stimulation

In addition to changes in the soluble mediator milieu, changes in the expression of cell surface markers by both immune and non-immune cell populations occur in PC, fostering a permissive tumor microenvironment (26). In particular, the down-regulation of HLA-I by PC cells and the up-regulation of tolerance-inducing costimulatory molecules such as PDL1 on multiple cells within the tumor microenvironment have been associated with aggressive disease and a poor prognosis (27). We have previously demonstrated that a TAS interferon response induced the expression of antigen presentation machinery in the context of negative co-stimulation (26). Thus, the effect of PCCM on the expression of both HLA ABC and PDL1 by TAS was assessed by flow cytometry. TAS from three different donors upregulated HLA ABC in a dose-dependent fashion in response to LPS treatment (Supplemental Fig. S2A). In contrast, the same TAS cultures did not upregulate HLA ABC as robustly, and sometimes not at all, in response to three different sources of PCCM (Supplemental Fig. S2B). Both LPS and PCCM induced the expression of PDL1 on TAS with similar efficacy (Supplemental Fig. S2, C and D). Again, there was variability in the robustness of the PDL1 response that appeared to be more dependent on the source of TAS rather than the source of PCCM (Supplemental Fig. S2D). Together these data indicate that the TAS may foster a pro-tumor environment in response to soluble mediators released by PC cells.

PCCM induces a TAS response that suppresses T cell proliferation and Th1 polarization

Using animal models, it has been demonstrated that the tumor microenvironment in PC suppresses antitumor immune responses through multiple mechanisms, including the suppression of $CD4^+$ T cell expansion and polarization, which can directly and indirectly inhibit cancer cell cytotoxicity (3). These mechanisms have not been fully elucidated in human PC, nor has the contribution of TAS to these mechanisms been evaluated. Thus, to explore the contribution of the PCCM-induced TAS secretory profile on adaptive immunity, TAS conditioned media (TAS CM) as a result of LPS ($TAS^{LPS}CM$) or PCCM ($TAS^{PC}CM$) pre-treatment was transferred to $CD3^+$ T cells isolated from a healthy donor (Fig. 5A). Polyclonal T cell stimulations were then performed and the proliferative capacity and immunophenotype (19) of resultant T cell populations evaluated. Unstimulated TAS CM suppressed both $CD4^+$ and $CD8^+$ T cell proliferation (Fig. 5B, C and D). However, $TAS^{LPS}CM$ (Fig. 5B and C) and $TAS^{PC}CM$ (Fig. 5B and D) resulted in further suppression of proliferation in a dose-dependent manner. Most importantly, both $TAS^{LPS}CM$ (Fig. 5E and F) and $TAS^{PC}CM$ (Fig. 5E and G) inhibited the expansion of Th1 T cells, as indicated by a reduction in the frequency of $CD4^+CXCR3^+$ cells. This inhibition was concomitant with the expansion of Th17 T cells, as indicated by an increase in the frequency of $CD4^+CCR6^+$ T cells (Fig. 5E, F and G). Finally, there was no effect on the expansion of $CD4^+FoxP3^+$ T regulatory cells regardless of TAS CM utilized (Fig. 5E, F and G). Neutralization of either IL6 or IL8 in $TAS^{PC}CM$ further reduced T cell suppression and Th1 polarization (Supplemental Fig. S3, A, B and C). Finally, MyD88 signaling in TAS was required for PCCM-induced stromal T cell suppression, as siRNA knockdown of either

MyD88 or IRAK1, but not TLR4, ameliorated stromal suppression of both T cell proliferation and Th1 polarization upon exposure to PCCM (Fig. 5H, Supplemental Fig. S3D).

In order to elucidate whether a similar phenomenon could be occurring *in vivo*, flow cytometric analysis of $CD4^+$ T cells in the peripheral blood of patients with PC and healthy controls was performed. Indeed, patients with PC presented with a higher frequency of $CD4^+$ effector memory cells ($CD45RA^-CCR7^-$) compared to healthy controls (Fig. 6A and B). While there was no significant difference in the frequency of Th1 effector memory cells ($CXCR3^+$) in the peripheral blood of patients with PC (Fig. 6A and C), these patients did exhibit a higher frequency of Th17 effector memory cells ($CCR6^+$) (Fig. 6, A and D), which resulted in an increased ratio of Th17/Th1 $CD4^+$ effector memory cells in the PC patient population (Fig. 6E). Together these data suggest that the MyD88-dependent response of TAS to soluble mediators from PC cells has the potential to promote Th17 immunity at the expense of Th1 immunity, an observation consistent with the adaptive immune phenotypes observed clinically in PC.

PCCM induces TAS responses that inhibit $CD8^+$ T cell-mediated killing of PC epithelial cells

Th1 cells can directly contribute to tumor immunity through cytokine production and CD95/CD95L-mediated killing of cancer cells (28,29). However, $CD8^+$ cytotoxic T cells (CTL) are thought to be primarily responsible for mediating antitumor immunity, while $CD4^+$ T cells provide help to antigen presenting cells, promoting complete licensing of $CD8^+$ T cell activation (28,29). Given this key role, there has been a large interest in mechanisms of tumor immune evasion from $CD8^+$ T cells (30,31). Thus, to evaluate the impact of PC-TAS interactions on $CD8^+$ T cell-mediated cytotoxicity, MART-1 tumor antigen-specific $CD8^+$ T cells were employed in a classical CTL assay (20). Specifically, MART-1 specific $CD8^+$ T cells were co-cultured with MART-1 pulsed primary PC cells in the presence of TAS conditioned media (TAS CM) or TAS CM pretreated with PCCM ($TAS^{PC}CM$) and cytotoxicity assessed (Fig. 7A). While TAS CM alone inhibited $CD8^+$ T cell antigen-specific killing of primary PC cells (Fig. 7B, C and D), again $TAS^{PC}CM$ induced a more robust inhibition of antigen-specific killing (Fig. 7B and C) even at high effector to target ratios (Fig. 7B and C). This inhibition of $CD8^+$ T cell cytotoxicity was associated with a statistically significant reduction in overall T cell proliferation (Fig. 7C). Both TAS CM and $TAS^{PC}CM$ also inhibited the production of IFNγ (Fig. 7E and H) and perforin (Fig. 7F and H), but not granzyme B (Fig. 7G and H) by the MART-1 specific T cells, with $TAS^{PC}CM$ again demonstrating higher efficacy (Fig. 7H). Together these data suggest that the MyD88-dependent response of TAS to soluble mediators from PC cells suppresses antigen-specific $CD8^+$ T cell effector function.

Discussion

Overcoming microenvironmental immune suppression is critical to developing successful immunotherapeutic strategies in PC. Proposed strategies to reverse tolerance include the inhibition of myeloid cell chemotaxis (32), licensing of antigen presenting cells (33),

regulatory T cell depletion (34), adjuvant approaches with vaccination (35) and others. However, despite preclinical successes, PC has proven resistant to traditional immune modulating therapies in the clinic (4). The mechanism(s) leading to what is now accepted to be a profoundly immunosuppressive microenvironment in human PC remain unclear. Considering the expansion and relative abundance of the myofibroblastic TAS component observed in PC, we hypothesized that these cells are actively contributing to this suppressive immune microenvironment. Thus, we leveraged primary human cell culture models derived from surgical specimens to evaluate the interaction between PC cells, TAS, and antitumor T cell populations in the human condition to delineate the soluble and cellular interactions impacting tumor immunity.

The relationship between PC cells and TAS continues to be an area of debate. TAS fuels PC cell proliferation, metastasis and treatment resistance, supporting a role as a tumor promoter (22). However, conditional stromal depletion techniques suggest the opposite relationship *in vivo*, demonstrating restraint of PC growth and metastasis by TAS (36,37). *Sherman et al.* demonstrated that modulation of TAS behavior, rather than its depletion, could effectively treat PC in preclinical models (38). Specifically, treatment with a vitamin D analogue led to a reduction in microenvironmental desmoplasia and ultimately prolonged survival in mice, suggesting that modulation of TAS behavior has the potential to restore an antitumor microenvironment (38). Data presented here also demonstrate an association between desmoplasia and the intratumoral soluble mediator microenvironment. Upon exposure to PC cell conditioned media, human TAS secrete IL6 and IL8 and upregulate antigen presentation machinery in the context of negative co-stimulation.

At this time, it is unclear which molecule(s) within the PC conditioned supernatants initiate this TAS innate immune response. Our data is clear that these DAMPs are heat labile molecules that can pass through a 0.2 um filter and engage receptors involved in MyD88-dependent signaling. While TLR4 activation fits these criteria and is sufficient to produce a suppressive TAS response, it does not appear to be required for the observed PCCM-induced TAS response, suggesting overlap of PCCM-induced alarmin signaling with other TLRs. The TAS response to pure TLR ligands would suggest the potential for TLR5 activity in addition to TLR4. However, endogenous DAMP responses may not always mirror those observed to commercially available TLR ligands, as we observed no TAS response to the recombinant TLR4 ligands, HMGB1 and β-defensin 2. Similar to our findings in PC, TLR4 activation in colonic stromal cells also induced T cell suppression via increased PDL1 expression (39). TLR4 expression in PC specimens has been shown to correlate with more aggressive disease (40) and it has been previously demonstrated that LPS-induced TLR4 signaling could be a trigger in the initiation and progression of PC (41). While it is clear from our studies that the phenomena observed are not due to LPS, multiple DAMPs are also known to engage TLRs (42) and identification of the ligand(s) within the primary PC cell conditioned media represents an active area of investigation for our laboratory.

Here we also demonstrate that exposure of TAS to PC cell conditioned media induces a milieu which can suppress the proliferation and induce the polarization of $CD4^+$ T cell populations to a more pro-tumor phenotype. The relationship between IL6, IL8 and Th17 polarization is well characterized. IL6, in addition to IL1β, TGFβ and IL23, can polarize T

cells toward a Th17 phenotype upon activation (43). The IL17 produced by Th17 cells then stimulates multiple cell types, including fibroblasts, to further secrete IL6 and IL8, promoting a positive feedback loop (44). On the other hand, the relevance of Th17 polarization in PC is controversial. *McAllister et al.* elegantly demonstrated that *k-ras* mutated ductal epithelial cells express functional IL17 receptors, which upon ligation further stimulate the development and progression of PanIN lesions (45). Alternatively, *Lutz et al.* and *Hiraoka et al.* both demonstrated correlations between Th17-associated gene expression in intratumoral tertiary lymphoid structures and improved prognosis in PC (46,47). Importantly, the context in which IL17 is expressed is key to its biological significance. In our model, TAS-induced Th17-polarization was accompanied by a loss of Th1 effector function, thus shifting the balance to a less robust antitumor response.

An effective anticancer response requires cytotoxic $CD8^+$ T cells and it has been demonstrated that patients with PC can generate $CD8^+$ T cells specific to antigens expressed on PC cells (7). When effector $CD8^+$ T cells can be detected in the tumor microenvironment it is generally thought to be a positive prognostic factor (48). However, upon progression of PC, $CD8^+$ T cells within the lesion decrease in number while the presence of $CD4^+$ regulatory T cells increases, suggesting that this transition is associated with escape from effective T cell immunity (2). In support of this, circulating $CD4^+$ T cells from patients with PC are associated with impaired function, favoring Th2 responses over Th1 (49). In addition to effects on $CD4^+$ T cell populations, the exposure of TAS to cancer cell conditioned media induced a milieu that directly suppressed antigen-specific cytotoxic function of $CD8^+$ T cells, associated with reduced IFNγ and perforin expression.

In summary, our findings using primary human tissues demonstrate an important role for PC-associated stroma in the suppression of intratumoral adaptive immunity. Given the relative abundance of TAS in the human disease, its capacity to directly and indirectly suppress T cell activation may have implications on the success of immune modulating therapies. Therefore, these data support strategies of stromal “reprogramming” in multimodal immunotherapeutic approaches to improve treatment outcomes in PC.

Supplementary Material

Refer to Web version on PubMed Central for supplementary material.

References

1. Rahib L, Smith BD, Aizenberg R, Rosenzweig AB, Fleshman JM, Matrisian LM. Projecting cancer incidence and deaths to 2030: the unexpected burden of thyroid, liver, and pancreas cancers in the United States. Cancer Res. 2014; 74(11):2913–2921. [PubMed: 24840647]
2. Clark CE, Hingorani SR, Mick R, Combs C, Tuveson DA, Vonderheide RH. Dynamics of the immune reaction to pancreatic cancer from inception to invasion. Cancer Res. 2007; 67(19):9518–9527. [PubMed: 17909062]
3. Winograd R, Byrne KT, Evans RA, Odorizzi PM, Meyer AR, Bajor DL, et al. Induction of T-cell Immunity Overcomes Complete Resistance to PD-1 and CTLA-4 Blockade and Improves Survival in Pancreatic Carcinoma. Cancer Immunol Res. 2015; 3(4):399–411. [PubMed: 25678581]

4. Royal RE, Levy C, Turner K, Mathur A, Hughes M, Kammula US, et al. Phase 2 trial of single agent Ipilimumab (anti-CTLA-4) for locally advanced or metastatic pancreatic adenocarcinoma. J Immunother. 2010; 33(8):828–833. [PubMed: 20842054]
5. Ridnour LA, Cheng RY, Switzer CH, Heinecke JL, Ambs S, Glynn S, et al. Molecular pathways: toll-like receptors in the tumor microenvironment--poor prognosis or new therapeutic opportunity. Clin Cancer Res. 2013; 19(6):1340–1346. [PubMed: 23271799]
6. Shalapour S, Karin M. Immunity, inflammation, and cancer: an eternal fight between good and evil. J Clin Invest. 2015; 125(9):3347–3355. [PubMed: 26325032]
7. Amedei A, Niccolai E, Prisco D. Pancreatic cancer: role of the immune system in cancer progression and vaccine-based immunotherapy. Hum Vaccin Immunother. 2014; 10(11):3354–3368. [PubMed: 25483688]
8. Bindea G, Mlecnik B, Tosolini M, Kirilovsky A, Waldner M, Obenauf AC, et al. Spatiotemporal dynamics of intratumoral immune cells reveal the immune landscape in human cancer. Immunity. 2013; 39(4):782–795. [PubMed: 24138885]
9. Zou W. Immunosuppressive networks in the tumour environment and their therapeutic relevance. Nat Rev Cancer. 2005; 5(4):263–274. [PubMed: 15776005]
10. Ye J, Livergood RS, Peng G. The role and regulation of human Th17 cells in tumor immunity. Am J Pathol. 2013; 182(1):10–20. [PubMed: 23159950]
11. Erkan M, Adler G, Apte MV, Bachem MG, Buchholz M, Detlefsen S, et al. StellaTUM: current consensus and discussion on pancreatic stellate cell research. Gut. 2012; 61(2):172–178. [PubMed: 22115911]
12. Sato Y, Goto Y, Narita N, Hoon DS. Cancer Cells Expressing Toll-like Receptors and the Tumor Microenvironment. Cancer Microenviron. 2009; 2(Suppl 1):205–214. [PubMed: 19685283]
13. Bhowmick NA, Neilson EG, Moses HL. Stromal fibroblasts in cancer initiation and progression. Nature. 2004; 432(7015):332–337. [PubMed: 15549095]
14. Abreu MT. Toll-like receptor signalling in the intestinal epithelium: how bacterial recognition shapes intestinal function. Nat Rev Immunol. 2010; 10(2):131–144. [PubMed: 20098461]
15. Han S, Delitto D, Zhang D, Sorenson HL, Sarosi GA, Thomas RM, et al. Primary outgrowth cultures are a reliable source of human pancreatic stellate cells. Lab Invest. 2015; 95(11):1331–1340. [PubMed: 26322418]
16. Delitto D, Pham K, Vlada AC, Sarosi GA, Thomas RM, Behrns KE, et al. Patient-derived xenograft models for pancreatic adenocarcinoma demonstrate retention of tumor morphology through incorporation of murine stromal elements. Am J Pathol. 2015; 185(5):1297–1303. [PubMed: 25770474]
17. Pham K, Delitto D, Knowlton AE, Hartlage ER, Madhavan R, Gonzalo DH, et al. Isolation of Pancreatic Cancer Cells from a Patient-Derived Xenograft Model Allows for Practical Expansion and Preserved Heterogeneity in Culture. Am J Pathol. 2016; 186(6):1537–1546. [PubMed: 27102771]
18. Delitto D, Black BS, Sorenson HL, Knowlton AE, Thomas RM, Sarosi GA, et al. The inflammatory milieu within the pancreatic cancer microenvironment correlates with clinicopathologic parameters, chemoresistance and survival. BMC Cancer. 2015; 15(1):783. [PubMed: 26498838]
19. Maecker HT, McCoy JP, Nussenblatt R. Standardizing immunophenotyping for the Human Immunology Project. Nat Rev Immunol. 2012; 12(3):191–200. [PubMed: 22343568]
20. Vatakis DN, Koya RC, Nixon CC, Wei L, Kim SG, Avancena P, et al. Antitumor activity from antigen-specific CD8 T cells generated in vivo from genetically engineered human hematopoietic stem cells. Proc Natl Acad Sci U S A. 2011; 108(51):E1408–E1416. [PubMed: 22123951]
21. Mitsunaga S, Ikeda M, Shimizu S, Ohno I, Furuse J, Inagaki M, et al. Serum levels of IL-6 and IL-1beta can predict the efficacy of gemcitabine in patients with advanced pancreatic cancer. Br J Cancer. 2013; 108(10):2063–2069. [PubMed: 23591198]
22. Erkan M, Hausmann S, Michalski CW, Fingerle AA, Dobritz M, Kleeff J, et al. The role of stroma in pancreatic cancer: diagnostic and therapeutic implications. Nat Rev Gastroenterol Hepatol. 2012; 9(8):454–467. [PubMed: 22710569]

23. Erkan M, Michalski CW, Rieder S, Reiser-Erkan C, Abiatari I, Kolb A, et al. The activated stroma index is a novel and independent prognostic marker in pancreatic ductal adenocarcinoma. Clin Gastroenterol Hepatol. 2008; 6(10):1155–1161. [PubMed: 18639493]
24. Garg AD, Martin S, Golab J, Agostinis P. Danger signalling during cancer cell death: origins, plasticity and regulation. Cell Death Differ. 2014; 21(1):26–38. [PubMed: 23686135]
25. Fitzgerald KA, Palsson-McDermott EM, Bowie AG, Jefferies CA, Mansell AS, Brady G, et al. Mal (MyD88-adapter-like) is required for Toll-like receptor-4 signal transduction. Nature. 2001; 413(6851):78–83. [PubMed: 11544529]
26. Delitto D, Perez C, Han S, Gonzalo DH, Pham K, Knowlton AE, et al. Downstream mediators of the intratumoral interferon response suppress antitumor immunity, induce gemcitabine resistance and associate with poor survival in human pancreatic cancer. Cancer Immunol Immunother. 2015; 64(12):1553–1563. [PubMed: 26423423]
27. Marincola FM, Jaffee EM, Hicklin DJ, Ferrone S. Escape of human solid tumors from T-cell recognition: molecular mechanisms and functional significance. Adv Immunol. 2000; 74:181–273. [PubMed: 10605607]
28. Brown DM, Kamperschroer C, Dilzer AM, Roberts DM, Swain SL. IL-2 and antigen dose differentially regulate perforin- and FasL-mediated cytolytic activity in antigen specific CD4+ T cells. Cell Immunol. 2009; 257(1–2):69–79. [PubMed: 19338979]
29. Williams NS, Engelhard VH. Perforin-dependent cytotoxic activity and lymphokine secretion by CD4+ T cells are regulated by CD8+ T cells. J Immunol. 1997; 159(5):2091–2099. [PubMed: 9278294]
30. Ueha S, Yokochi S, Ishiwata Y, Ogiwara H, Chand K, Nakajima T, et al. Robust anti-tumor effects of combined anti-CD4 depleting antibody and anti-PD-1/PD-L1 immune checkpoint antibody treatment in mice. Cancer Immunol Res. 2015
31. Kalathil SG, Thanavala Y. High immunosuppressive burden in cancer patients: a major hurdle for cancer immunotherapy. Cancer Immunol Immunother. 2016
32. Sanford DE, Belt BA, Panni RZ, Mayer A, Deshpande AD, Carpenter D, et al. Inflammatory monocyte mobilization decreases patient survival in pancreatic cancer: a role for targeting the CCL2/CCR2 axis. Clin Cancer Res. 2013; 19(13):3404–3415. [PubMed: 23653148]
33. Beatty GL, Chiorean EG, Fishman MP, Saboury B, Teitelbaum UR, Sun W, et al. CD40 agonists alter tumor stroma and show efficacy against pancreatic carcinoma in mice and humans. Science. 2011; 331(6024):1612–1616. [PubMed: 21436454]
34. Soares KC, Rucki AA, Kim V, Foley K, Solt S, Wolfgang CL, et al. TGF-beta blockade depletes T regulatory cells from metastatic pancreatic tumors in a vaccine dependent manner. Oncotarget. 2015
35. Keenan BP, Saenger Y, Kafrouni MI, Leubner A, Lauer P, Maitra A, et al. A Listeria vaccine and depletion of T-regulatory cells activate immunity against early stage pancreatic intraepithelial neoplasms and prolong survival of mice. Gastroenterology. 2014; 146(7):1784–1794. e6. [PubMed: 24607504]
36. Ozdemir BC, Pentcheva-Hoang T, Carstens JL, Zheng X, Wu CC, Simpson TR, et al. Depletion of carcinoma-associated fibroblasts and fibrosis induces immunosuppression and accelerates pancreas cancer with reduced survival. Cancer Cell. 2014; 25(6):719–734. [PubMed: 24856586]
37. Rhim AD, Oberstein PE, Thomas DH, Mirek ET, Palermo CF, Sastra SA, et al. Stromal elements act to restrain, rather than support, pancreatic ductal adenocarcinoma. Cancer Cell. 2014; 25(6): 735–747. [PubMed: 24856585]
38. Sherman MH, Yu RT, Engle DD, Ding N, Atkins AR, Tiriac H, et al. Vitamin d receptor-mediated stromal reprogramming suppresses pancreatitis and enhances pancreatic cancer therapy. Cell. 2014; 159(1):80–93. [PubMed: 25259922]
39. Beswick EJ, Johnson JR, Saada JI, Humen M, House J, Dann S, et al. TLR4 activation enhances the PD-L1-mediated tolerogenic capacity of colonic CD90+ stromal cells. J Immunol. 2014; 193(5):2218–2229. [PubMed: 25070848]
40. Zhang JJ, Wu HS, Wang L, Tian Y, Zhang JH, Wu HL. Expression and significance of TLR4 and HIF-1alpha in pancreatic ductal adenocarcinoma. World J Gastroenterol. 2010; 16(23):2881–2888. [PubMed: 20556833]

41. Daniluk J, Liu Y, Deng D, Chu J, Huang H, Gaiser S, et al. An NF-kappaB pathway-mediated positive feedback loop amplifies Ras activity to pathological levels in mice. J Clin Invest. 2012; 122(4):1519–1528. [PubMed: 22406536]

42. Erridge C. Endogenous ligands of TLR2 and TLR4: agonists or assistants? J Leukoc Biol. 2010; 87(6):989–999. [PubMed: 20179153]

43. Hu W, Troutman TD, Edukulla R, Pasare C. Priming microenvironments dictate cytokine requirements for T helper 17 cell lineage commitment. Immunity. 2011; 35(6):1010–1022. [PubMed: 22137454]

44. Lee JW, Wang P, Kattah MG, Youssef S, Steinman L, DeFea K, et al. Differential regulation of chemokines by IL-17 in colonic epithelial cells. J Immunol. 2008; 181(9):6536–6545. [PubMed: 18941244]

45. McAllister F, Bailey JM, Alsina J, Nirschl CJ, Sharma R, Fan H, et al. Oncogenic Kras activates a hematopoietic-to-epithelial IL-17 signaling axis in preinvasive pancreatic neoplasia. Cancer Cell. 2014; 25(5):621–637. [PubMed: 24823639]

46. Lutz ER, Wu AA, Bigelow E, Sharma R, Mo G, Soares K, et al. Immunotherapy converts nonimmunogenic pancreatic tumors into immunogenic foci of immune regulation. Cancer Immunol Res. 2014; 2(7):616–631. [PubMed: 24942756]

47. Hiraoka N, Ino Y, Yamazaki-Itoh R, Kanai Y, Kosuge T, Shimada K. Intratumoral tertiary lymphoid organ is a favourable prognosticator in patients with pancreatic cancer. Br J Cancer. 2015; 112(11):1782–1790. [PubMed: 25942397]

48. Tewari N, Zaitoun AM, Arora A, Madhusudan S, Ilyas M, Lobo DN. The presence of tumour-associated lymphocytes confers a good prognosis in pancreatic ductal adenocarcinoma: an immunohistochemical study of tissue microarrays. BMC Cancer. 2013; 13:436. [PubMed: 24063854]

49. De Monte L, Reni M, Tassi E, Clavenna D, Papa I, Recalde H, et al. Intratumor T helper type 2 cell infiltrate correlates with cancer-associated fibroblast thymic stromal lymphopoietin production and reduced survival in pancreatic cancer. J Exp Med. 2011; 208(3):469–478. [PubMed: 21339327]

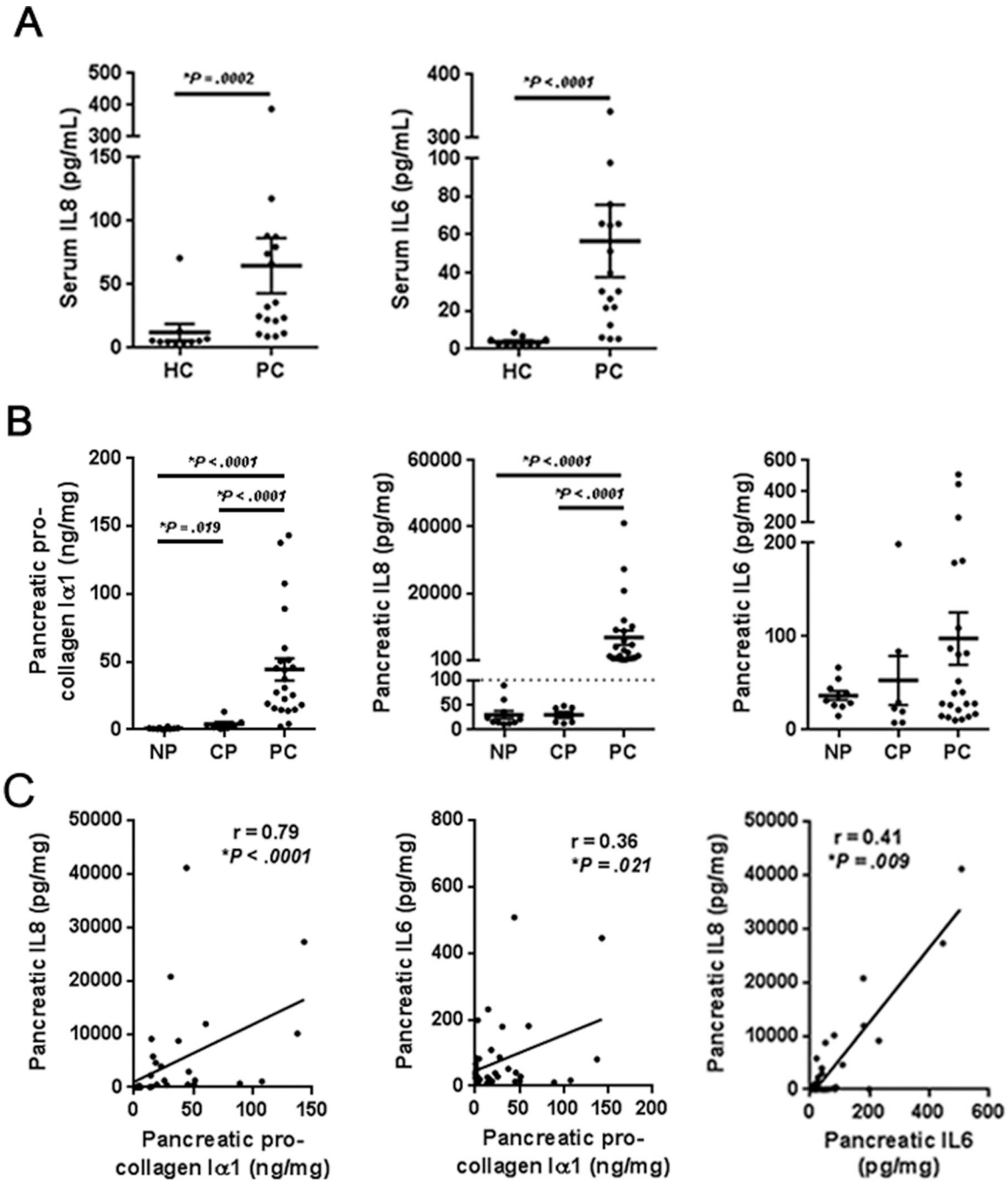

Figure 1. Local IL6 and IL8 expression correlate with desmoplasia in pancreatic cancer

A, plasma IL8 and IL6 concentrations in healthy controls (HC, n=10) and patients with resectable pancreatic cancer (PC, n=18). B, pro-collagen Iα1, IL8 and IL6 concentrations in pancreatic surgical specimens from normal pancreas (NP, n=10), chronic pancreatitis (CP, n=7) and pancreatic cancer (PC, n=23). C, mediators were correlated using spearman's rank correlation coefficients. Bars represent mean ± S.E.M. *$P < 0.05$ using the Mann Whitney U test.

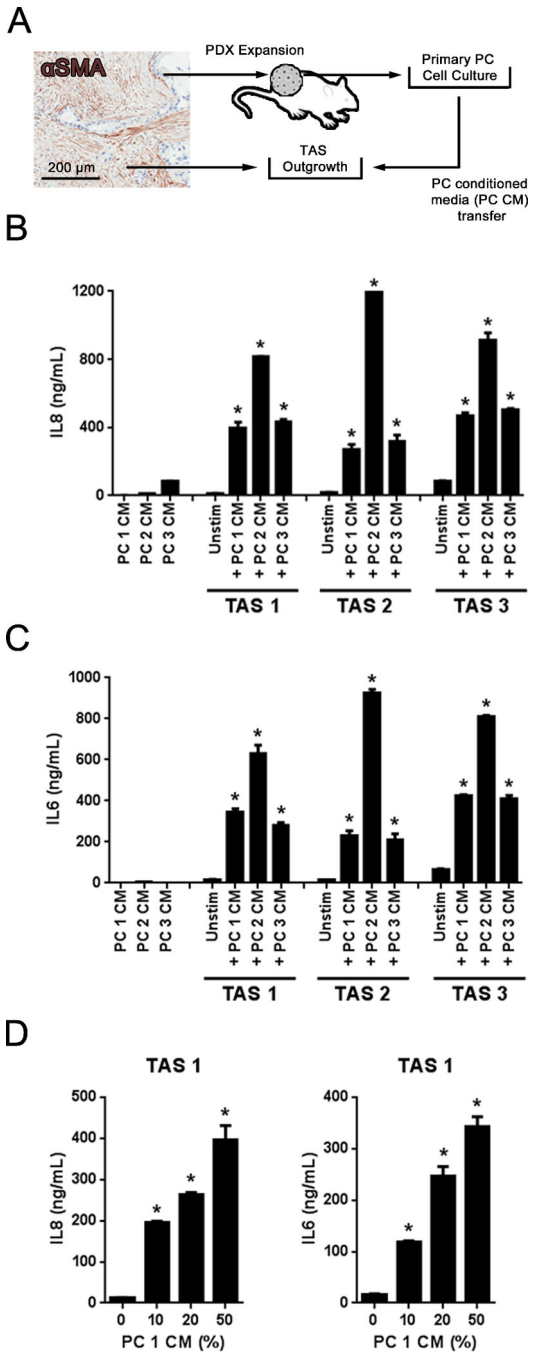

Figure 2. Primary tumor-associated stroma cultures secrete IL8 and IL6 in response to primary pancreatic cancer cell conditioned media

A, micrograph demonstrating αSMA-positive (brown) desmoplasia associated with PC. Primary tumor-associated stromal cells (TAS) were cultured from PC specimens and PC cells were isolated and expanded from patient-derived xenografts. TAS cells were treated with conditioned media from primary PC cells (PCCM). B and C, IL8 and IL6 in PCCM as well as the supernatants resulting from 24 hours of exposure or not to 50% dilution of PCCM. D, Dose response of IL8 and IL6 expression by TAS upon exposure to PCCM. Bars

represent mean ± S.E.M. *$P < .05$ compared to unstimulated (unstim) using the independent samples *t* test.

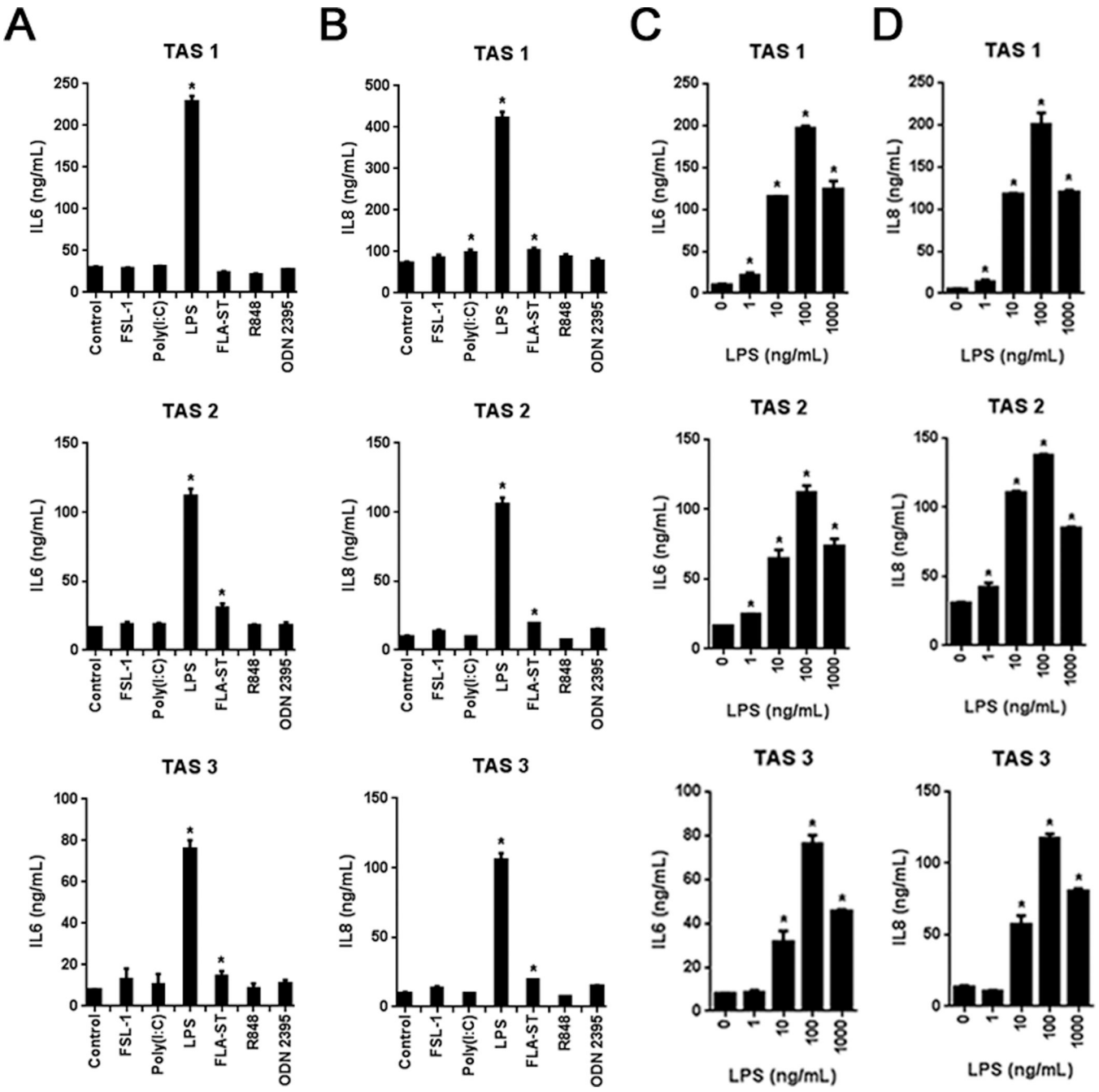

Figure 3. TAS secretory response is specific to TLR4 and TLR5 stimulation

A and B, IL6 and IL8 expression in TAS exposed to 100 ng/ml of the indicated pattern recognition receptor (PRR) agonists. C and D, TAS expression of IL6 and IL8 following exposure to ultrapure LPS at the indicated doses. Bars represent mean ± S.E.M. $*P < 0.05$ compared to controls using the independent samples *t* test.

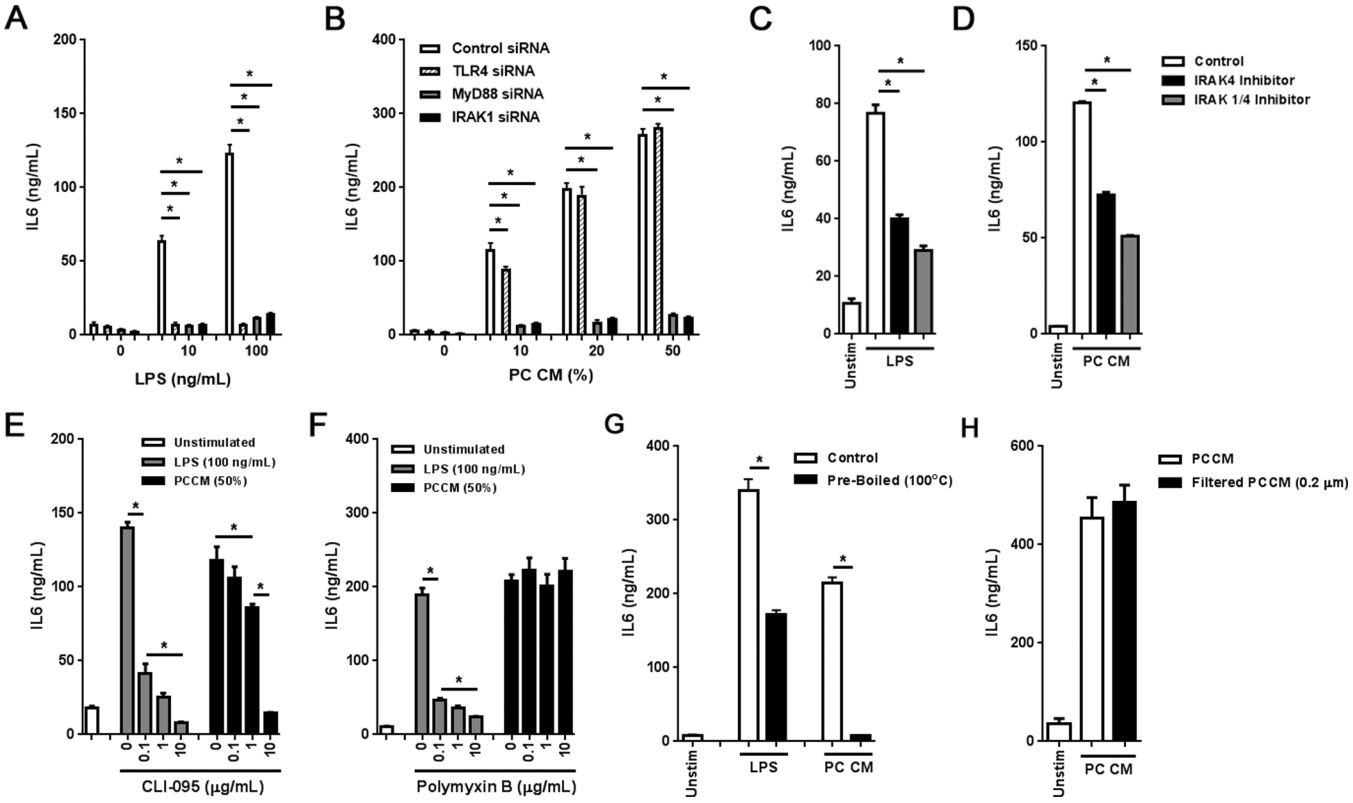

Figure 4. TAS secretion of IL6 and IL8 in response to PCCM is MyD88-dependent

A and B, TAS was treated with siRNA specific to TLR4, MyD88, IRAK1 or control siRNA and exposed to (A) ultrapure LPS as well as (B) PCCM and IL6 secretion evaluated. C and D, IL6 secretion by TAS following exposure to (C) 100 ng/mL of ultrapure LPS or (D) PCCM (50%) in the presence of 10 μM of a small molecule IRAK4 inhibitor (black) or 10 μM of a small molecule inhibitor specific to both IRAK1 and IRAK4 (gray). E and F, IL6 secretion by TAS treated with ultrapure LPS (100 ng/mL, gray) or PCCM (50%, black) was evaluated in the presence of (E) the TLR4 inhibitor, CLI-095, or (F) polymyxin B. G, IL6 secretion by TAS exposed to 100 ng/mL of ultrapure LPS or PCCM (50%) with (black) and without pre-boiling (white). H, IL6 secretion by TAS exposed to filtered (black) or non-filtered (white) PC conditioned media (50%). Bars represent mean ± S.E.M. *$P < 0.05$ using the independent samples *t* test.

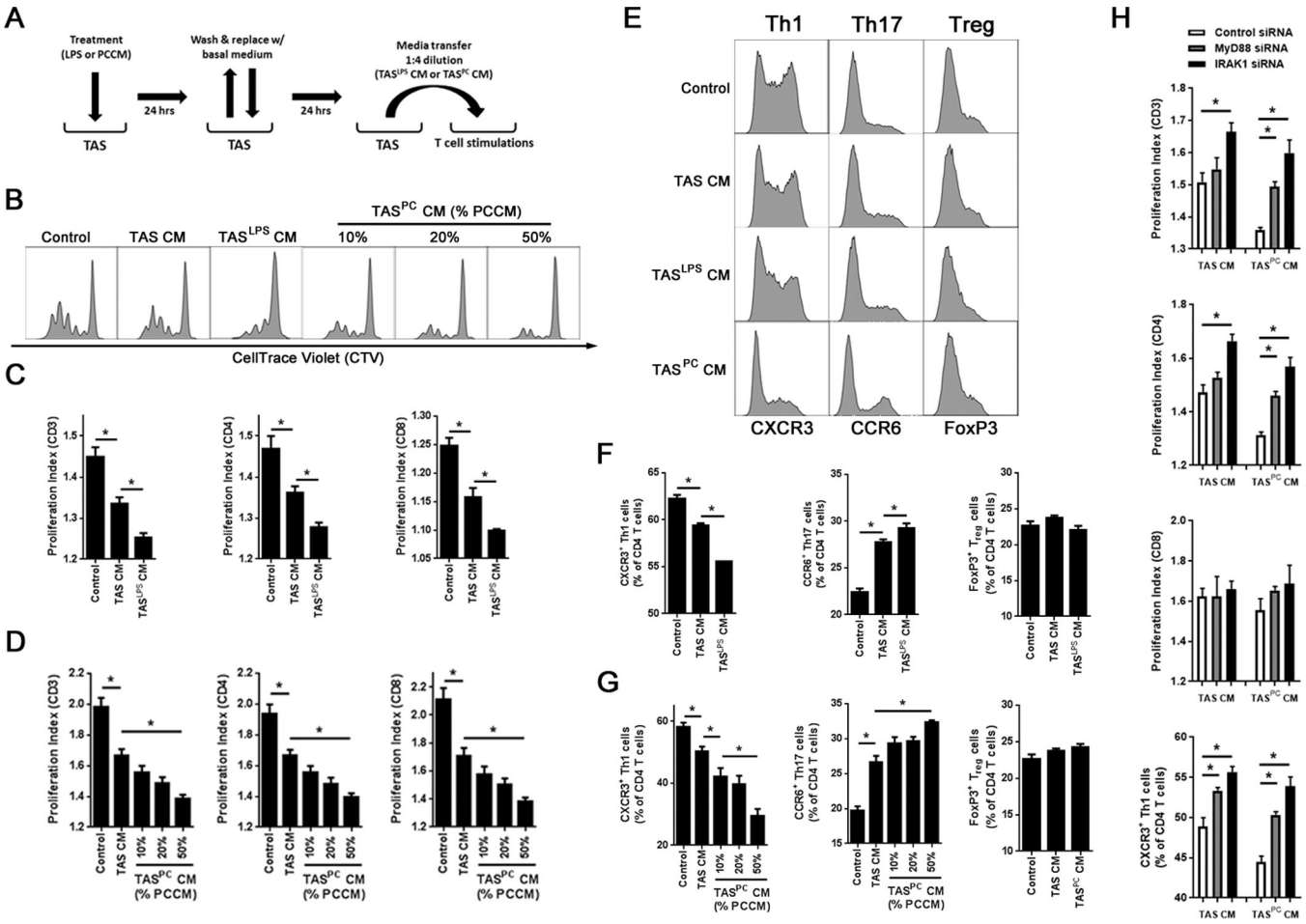

Figure 5. The TAS innate immune response to pancreatic cancer conditioned media or TLR4 stimulation suppresses and polarizes adaptive immunity in a MyD88-dependent manner

A, TAS cultures were treated for 24 hours with either 100 ng/ml of ultrapure LPS or PCCM (50%). Cells were then washed and returned to fresh growth medium for an additional 24 hours. Conditioned media from TAS was then transferred to magnetically sorted, CellTrace™ Violet (CTV)-stained T cells from a healthy volunteer at a 1:4 dilution (20%) in growth medium. T cells were stimulated with anti-CD3/CD28/CD137 beads for four days in the presence of IL2 (50 U/mL). B, representative histograms evaluating T cell proliferation via CTV dilution for control T cells, TAS conditioned media (TAS CM)-treated T cells, LPS pretreated TAS CM-treated T cells (TAS^{LPS} CM), or PCCM pretreated (10%, 20% or 50% PCCM) TAS CM-treated T cells (TAS^{PC} CM). C and D, proliferation indices for total T cells (CD3), CD4, and CD8 T cells were calculated for (C) TAS^{LPS} CM and (D) TAS^{PC} CM. (E) Representative histograms for CD4 T cells expressing CXCR3 (Th1), CCR6 (Th17) or FoxP3 (T_{reg}). F and G, percentage of CD4 T cells with a Th1, Th17 and T_{reg} phenotype were quantified after stimulation in the presence of (F) TAS^{LPS} CM and (G) TAS^{PC} CM groups. H, T cell stimulations were performed using conditioned media generated from TAS after siRNA knockdown of MyD88, IRAK1 or control siRNA. Proliferation indices of CD3, CD4 and CD8 T cells are displayed as well as Th1 polarization. Bars represent mean ± S.E.M. $*P < 0.05$ using the independent samples *t* test.

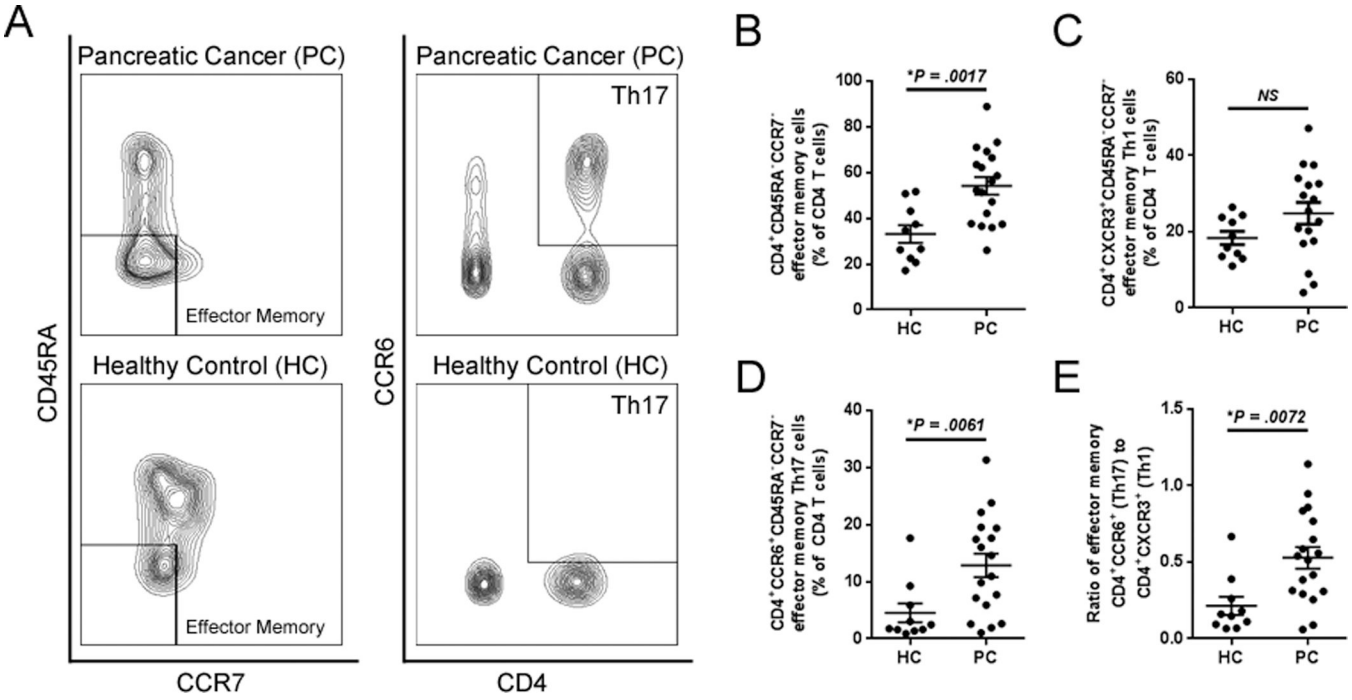

Figure 6. Th17 polarization of systemic effector memory T cells in patients with PC

A, representative contour plots of peripheral blood T cells (gated on live $CD3^+$ cells) evaluated for $CD45RA^-CCR7^-$ effector memory phenotypes as well as $CD45RA^-CCR7^-CD4^+CCR6^+$ effector memory Th17 cells. B, circulating $CD45RA^-CCR7^-$ effector memory T cells were quantified in patients with pancreatic cancer (PC, n=18) vs. healthy controls (HC, n=10). C and D, the frequency of effector memory T cells polarized toward (C) Th1 or (D) Th17 as well as (E) the ratio of Th17/Th1 effector memory cells were quantified. Bars represent mean ± S.E.M. $*P < 0.05$ using the Mann Whitney U test.

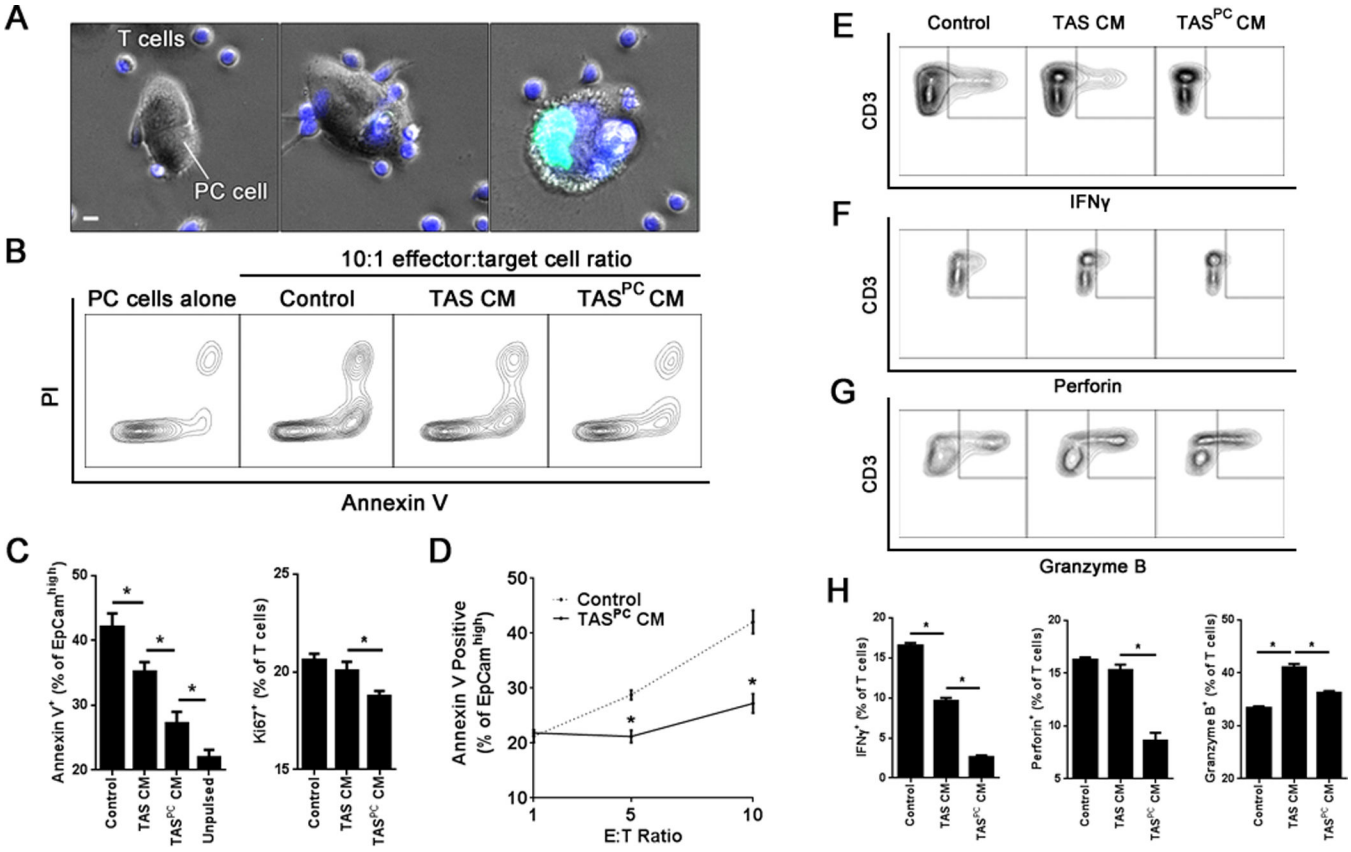

Figure 7. The stromal innate immune response to pancreatic cancer suppresses antitumor T cell-mediated lymphotoxicity

A, transgenic HLA-A2, MART1-specific CD8 T cells were labeled with CellTracker Blue (blue) and co-cultured with MART1-pulsed primary PC cells in the presence of SYTOX® Green (green). Representative images of co-cultures are displayed. Scale bar indicates 5 μm. B, representative contour plots evaluating apoptosis at 24 hours in EpCam^{high} PC cells using annexin V and propidium iodide (PI) stains. C, quantification of annexin-positive apoptotic cancer cells (*left*) and Ki67-positive proliferating CD8^{+} T cells (*right*) under each indicated condition at a 10:1 effector:target (E:T) cell ratio. Unpulsed cells indicate the absence of exogenous MART1 peptide and thus served as a negative control. D, PC cell apoptosis was evaluated at the indicated E:T cell ratios for both control and PCCM-stimulated TAS CM (TAS^{PC} CM) conditions. Representative contour plots of (E) IFNγ, (F) perforin and (G) granzyme B expression in T cells as well as (H) quantification of each population for the indicated conditions at a 10:1 E:T ratio. Bars represent mean ± S.E.M. *$P < 0.05$ using the independent samples *t* test.